

Considerations for Scale-Up of Ferronickel Electric Smelting Furnaces

R.J. HUNDERMARK^{1,3} and L.R. NELSON²

1.—Anglo American, Johannesburg, South Africa. 2.—Anglo American Platinum, Johannesburg, South Africa. 3.—e-mail: rodney.hundermark@angloamerican.com

In ferronickel smelting, the selective carbothermic reduction of calcined nickel laterite ores in large electric furnaces yields a crude ferronickel product. The optimal process for nickel laterite smelting requires a fine balance between the metallurgical requirements of the process (feed composition, nickel recovery, energy consumption, product quality) and the capabilities of the feeding, tapping and off-gas systems, and especially of the furnace crucible and electrical system. The scale-up of nickel laterite smelting operations over the last 50 years has seen a tenfold increase in furnace power input. Furnace operations within the industry are examined to identify common trends and some new metrics are proposed which incorporate the combination of electrode power densities and the impact of alloy nickel grade on gas generation rates, and hence local electrode gas fluxes, which may impact on future scale-up of ferronickel furnaces.

INTRODUCTION

Pyrometallurgical treatment of nickel laterite ores typically entails partial drying of the ore, further drying and calcination of the ore in rotary kilns, followed by smelting in large electric furnaces [termed the rotary kiln–electric furnace (RKEF) process] to produce a ferronickel product. Fifty years ago, the power rating on ferronickel electric furnaces was ~10 MW. The industry has advanced significantly since then, with power input into modern day electric furnaces having increased tenfold,¹ and currently there exists a ferronickel furnace with a maximum power rating slightly exceeding 100 MW. Extrapolation of the maximum capacities of ferronickel smelting furnaces has been considered previously, where it has been suggested that a 120-MW furnace is possible,² and that, for an alternating current (AC) furnace, a power input of 150 MW may even be plausible based on proven metrics on existing furnaces.¹

From the 1970s onwards, the shielded arc mode of electrode operation was introduced,³ in which an arc is drawn between the electrode tip and the slag, and the arc is covered with feed calcine. This was quantified electrically by describing the total electrode power in terms of a ratio of arc power to bath power ($P_{\text{arc}}/P_{\text{bath}}$), with the assumption of a

pervasive presence of stable calcine burden to ‘shield’ the arc portion above the liquid bath at all times. This, together with higher intensity furnace sidewall cooling, provided a breakthrough for increasing the power input on ferronickel furnaces through operating at higher hearth power densities than traditional immersed electrode operations (typically < 200 kW/m²). In this manner nickel output from essentially the same size furnace has significantly increased.^{2,4}

Based on literature information,^{2,5–7} the hearth power densities of several ferronickel furnaces have been expressed in a plot of maximum and nominal power versus hearth cross-sectional area (Fig. 1). With the exception of the furnaces at Falcondo and PT Vale/Inco (PTV), none of the other operations have operated sustainably at levels significantly above hearth power densities of ~250 kW/m², despite having the electrical, and crucible cooling systems to do so. It is therefore suggested that the hearth power density may not be the actual limiting factor in other operations, and other aspects need to be considered. The significance of the hearth power density lines and mode of electrode operation (open arc, submerged arc, shielded arc, immersed) for ferronickel and other commodities, has been explored in more detail elsewhere.⁸

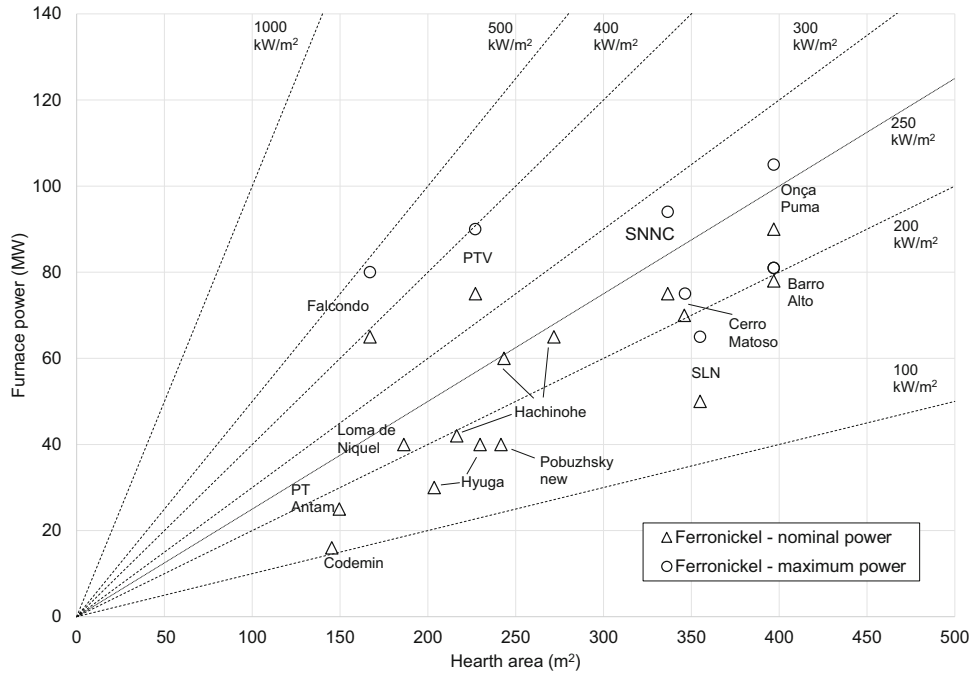


Fig. 1. Furnace power versus hearth area for ferronickel furnaces.

OTHER FERRONICKEL SMELTING ASPECTS

The furnaces at Cerro Matoso, Falcondo and PTV have historically stood out in terms of power density, and more recently the furnaces at Posco SNNC, Onça Puma and Barro Alto have been approaching similar hearth power densities. The power input per electrode has been a metric cited^{1,2} in extrapolation of possible future furnace power ratings (Fig. 2). Operation of the circular, three-electrode furnaces at Cerro Matoso, SNNC and PTV has proven power inputs of 25 MW per electrode. A further refinement of this metric was suggested for consideration,¹ that being the electrode power density (power per electrode/electrode cross-sectional area), where for a 1.8-m diameter, the 25-MW power input per electrode yields an electrode power density of 9.8 MW/m² (Fig. 3). It is noted that Falcondo operated with pre-baked electrodes of 1 m diameter,⁹ which have a higher electrode power density (about 13 MW/m²). However, the electrode power density itself may well be a proxy for another factor, which is that of local electrode gas generation rate, which is additionally dependent on the quality of calcine smelted, nickel grade being produced and the specific mode of electrode operation.

Ferronickel is produced at a range of alloy nickel grades from 15% to 40%, with the grade depending on a number of factors including geographical location and economics for overall nickel and iron recovery.^{10,11} The ferronickel product grade is a function of the feed ore nickel grade, Fe:Ni ratio,

and the degree of iron reduction/recovery. The extent of iron reduction can be grouped into two ranges, namely a low degree of iron recovery (10–30%) and a high degree of iron recovery (45–70%). Based on data for industrial ferronickel smelters,⁵ it is observed that there is the expected correlation between the nickel recovery and iron recovery (Fig. 4), and distinct groupings of the low and high iron recovery operations. A pragmatic approach¹² for relating the nickel and iron recoveries utilizes a convenient thermodynamic lumped activity coefficient parameter ($K\gamma$) which is illustrated for values of 20, 30 and 50 (a $K\gamma$ value of 20 has been suggested based on direct current pilot scale ferronickel smelting test work¹³). $K\gamma$ generically describes recovery of a metal to alloy (e.g., nickel) from its oxide in the slag, relative to the recovery of iron from that slag, through the relevant exchange reaction equilibrium constant K (a function of temperature only) and the overall ratio of metal and slag activity coefficients (involving individual γ values). The results of thermodynamic modeling^{11,14} predict higher nickel recoveries for specified iron recoveries than is typically achieved industrially, and the “non-equilibrium” behavior of Ni, Si and C in ferronickel smelting with high iron recovery is noted; however, will not be explored further here. Silicon reversion,¹⁵ in which silicon reduced to the metal phase reacts with the oxides in the slag phase thereby generating significant energy, is a known phenomenon in furnaces producing lower grade ferronickel, but will also not be explored further here.

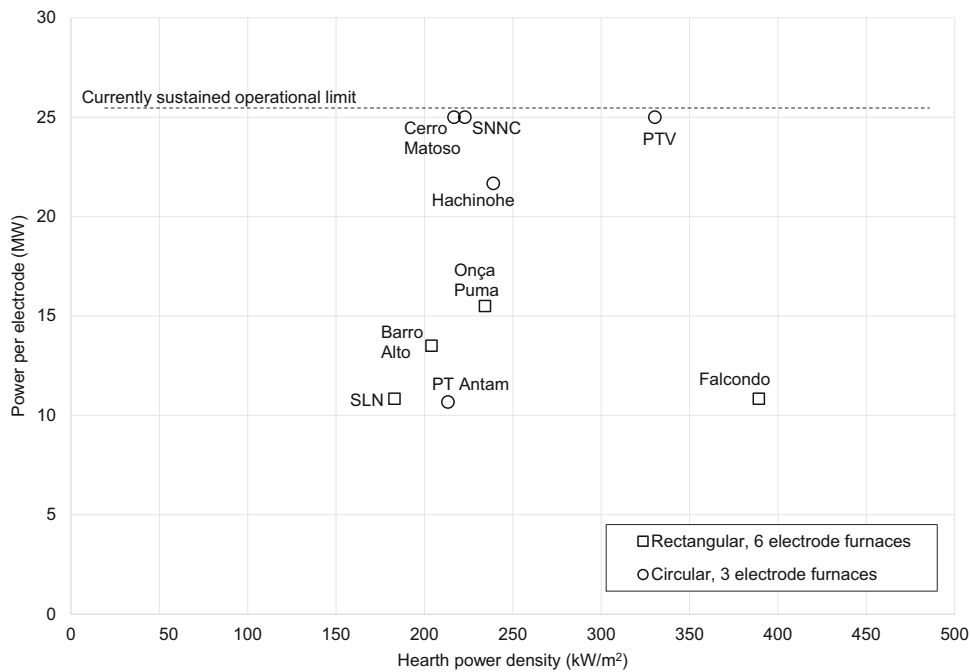


Fig. 2. Power per electrode for high power density furnace operations (vs. prevailing 31.3 MW/electrode SNNC design limit).

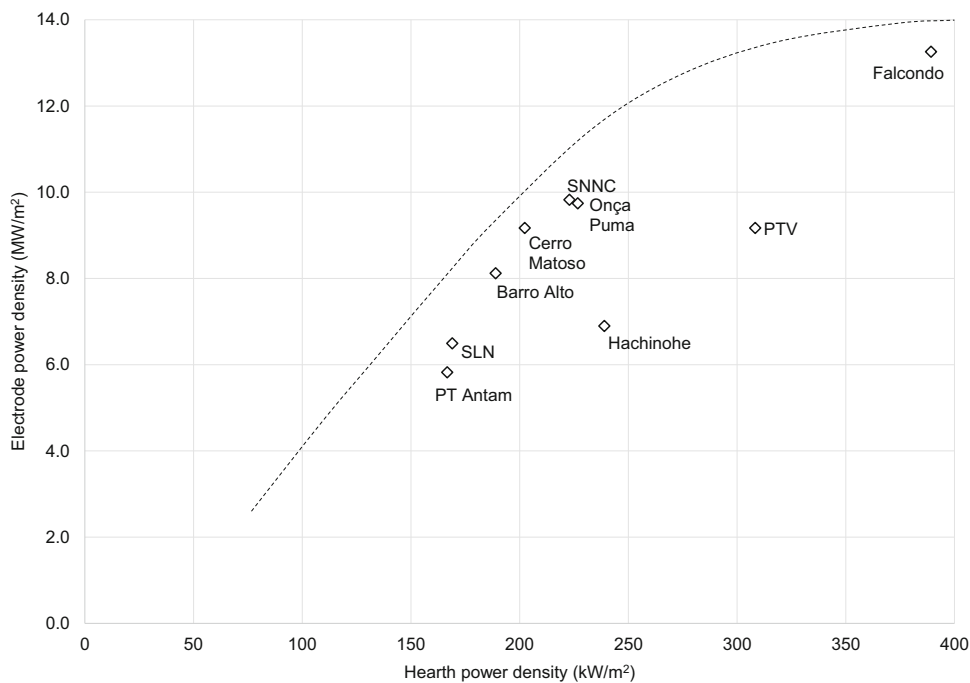


Fig. 3. Electrode power density associated with equivalent hearth power density for high power furnaces.

Previous analysis^{16,17} has provided insight into the overall gas generation in the furnace as a function of nickel grade, and noted that the local gas generation around the electrodes is important. In particular, Walker et al.¹⁷ note that, as the electrode operation moves from immersed mode to shielded

arc mode, and power input shifts from bath power to arc power, so the energy input becomes more concentrated around the electrodes, and it is suggested that 90% of the calcine will be consumed in the “center zone” of the furnace. Given that the temperatures in the arc zone are hottest, and most

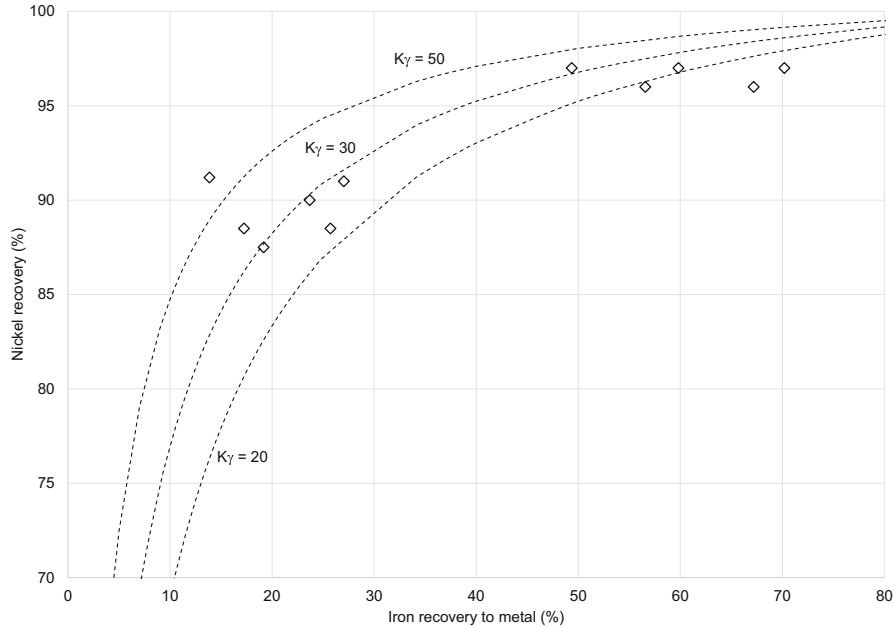


Fig. 4. Relationship between nickel recovery and iron recovery in ferronickel smelting.

of the feed will be consumed in this localized area, the rate and volume of gas generation in the arc zone is likely to be highest.

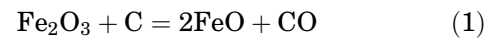
With production of lower alloy nickel grades, requiring higher degrees of iron reduction and correspondingly higher gas generation rates, the quantity of gas generated in the arc zone increases. The risk that this introduces is that the calcine pile shielding the arc may be blown away by the volume of gas generated in the arc zone (described as “burners” in one instance,¹⁸ and see examples in Nelson et al.¹⁵), leading to excessively high roof and freeboard temperatures. Especially when combined with any local excess of reductant, this may even start to drive highly endothermic MgO and SiO₂ reduction reactions (potentially leading to gaseous Mg(g) and SiO(g) intermediate products); an undesirable operating condition for most ferronickel furnaces.

Several options would exist for remedying the situation, including: reduction of power thereby reducing gas generation rate; increasing degree of pre-reduction achieved in the RK; increasing feed pile heights around the electrode (although this may further complicate the issue by not allowing sufficient gas to escape, leading to pressure build-up below a solid crust); moving towards brush arc or an immersed mode of electrode operation; or decreasing the overall extent of electric furnace reduction (lowering nickel and iron recovery, so increasing the alloy nickel grade). With the exception of increasing the degree of reduction in the rotary kiln, none of the other options are particularly attractive in simultaneously promoting both nickel alloy yield and smelting productivity.

ASSESSMENT OF LOCAL ELECTRODE GAS GENERATION

On the basis that local electrode gas generation rates are likely a constraint in ferronickel smelting, somewhat more quantitative metrics have been developed, as follows:

- Depending on the alloy nickel grade to be produced at a particular smelting operation, the quantity of gas that is generated in the furnace is inversely related to the nickel grade. This is a direct function of the metal oxide reduction reactions needing to take place in the furnace which require carbon addition, offset by the degree of pre-reduction obtained (e.g., in the rotary kiln for a RKEF configuration). The reactions between NiO and alloy and the Boudouard reaction are also important; however, the calculations below consider only the potential carbon monoxide reaction gas formed through carbothermic reduction of nickel and iron oxides locally around the electrode. On release from around the electrode, the CO gas will tend to combust with the oxygen in the ingress air entering the furnace to form CO₂; however, this additional gas volume is not considered in the local electrode gas volume calculations.



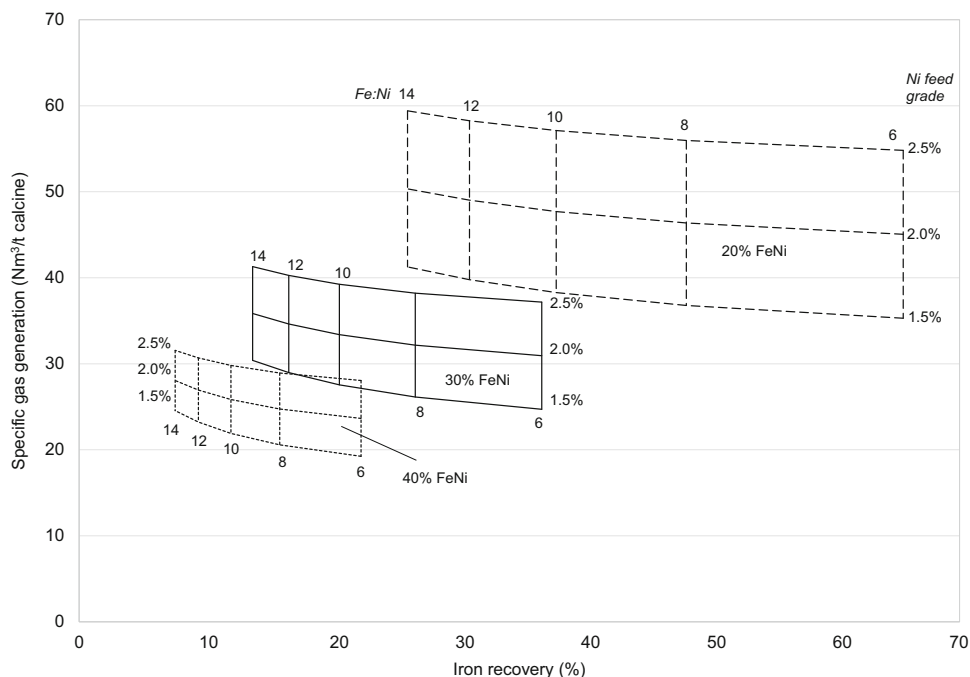


Fig. 5. Specific gas generation per ton of calcine (Nm^3/t) as a function of iron recovery, linked to nickel feed grade (horizontal lines), feed Fe:Ni ratio (vertical lines) and alloy nickel grade.

- In order to provide some illustrative guidance on the magnitude of the differences in gas generation between high and low iron recovery operations (low and high alloy nickel grade, respectively), theoretical calculations were carried out considering reduction of calcine of varying Fe:Ni ratios and feed Ni grades at a range of iron recoveries (Fig. 5). Note that this analysis assumes that 50% of the pre-reduction of Fe^{3+} to Fe^{2+} occurs in the kiln and the remainder of calcine reduction takes place in the electric furnace (EF). The extent of nickel reduction required is linked to the iron recovery based on a $K\gamma$ value of 30.
- Fully dried and calcined RK product are assumed, so making negligible further contribution to EF gas evolution. Resultant gas volumes are expressed at normal temperature and pressure (273.15 K and 101.325 kPa) for convenience, although this may not strictly account for fully comparing conditions of differing electrode reaction zone temperatures.

The quantity of gas generated per ton of calcine is a strong function of the extent of iron reduction as expected, and is less affected by the ore feed nickel grade. Almost twice as much gas is generated for producing ferronickel at an alloy grade of 20% Ni than for producing ferronickel at double the alloy grade of 40% Ni, for the same feed nickel grade and Fe:Ni ratio.

ESTIMATION OF LOCAL ELECTRODE GAS FLUX

In order to relate the quantity of gas generated per ton of calcine to the conditions around an electrode, a local electrode gas flux (can also be

expressed as a superficial gas velocity) is proposed. Assuming that the majority of the feed into the furnace is consumed in the active electrode zone (utilizing the assumption of 90% smelted in the “center zone”), the quantity of gas generated within this area around the electrode can be calculated as a function of calcine composition, specific EF energy consumption (assumed to be 0.5 MWh/t calcine) and degree of pre-reduction in the rotary kiln (50% as noted above), and expressed as a flux.

The following was considered in attempting to quantify the area around the electrode through which the gas is released:

- Based on visual observations on several ferronickel furnaces, gas appears preferentially released in close proximity to the electrodes, and the CO emitted combusts, producing flames when exposed to the oxidizing freeboard gas.
- Assuming the presence of a paraboloid of power dissipation, and/or similarly shaped arc cavity or crater (see Refs. 19 and 20) between the electrode and the slag, the shortest path (lowest pressure drop) for gas to escape from around the arc cavity will be directly adjacent to the electrodes where there is a lower height of calcine above the cavity.
- Given the highest relative movement between the calcine and the electrode, the voidage in the calcine is also likely to be highest directly around the electrode, which would further enhance gas flow in this area.
- On this basis, it has been estimated that the gas local to the electrode is likely released in a ring of about twice the electrode diameter ($2D_e$) around

each electrode. The cross-sectional area of this annulus is thus 3 times the cross-sectional area of the electrode. Given typical electrode spacings on most furnaces of $\sim 2.5 D_e$, the local gas flux areas of adjacent electrodes as assumed do not touch or overlap.

Based on the gas generation rate information (Fig. 5), the electrode gas flux ($\text{Nm}^3/\text{h}/\text{m}^2$) is first plotted as a function of the alloy nickel grade for several industrial operations for their specific feed and ferronickel product compositions (Fig. 6). The correlation between the higher gas flux and lower alloy nickel grade is noted and expected.

INFLUENCE OF ELECTRODE POWER DENSITY ON LOCAL ELECTRODE GAS FLUX

To illustrate the combined effects of both electrode diameter and power input, the electrode gas flux is plotted versus the electrode power density (Fig. 7). To simplify the representation for the trend lines, this is done for the 20%, 30% and 40% alloy nickel grade ranges, but only for a feed nickel grade of 2% and at a Fe:Ni feed ratio of 8. As expected, electrode gas flux is projected to increase roughly linearly with electrode power density, while the gradient increases with decreasing alloy nickel grade, indicative of increasing electrode gas flux.

Data for industrial operations are superimposed (based on available literature information and estimates of some variables, particularly degree of pre-reduction, where not explicitly available), which show:

- The Falcondo furnace is potentially the best example of where shielded arc operation permit-

ted substantially increased power on the same size furnace footprint. Despite the very high electrode power density (up to $13 \text{ MW}/\text{m}^2$), the estimated electrode gas flux is lowest at $\sim 125 \text{ Nm}^3/\text{h}/\text{m}^2$. This is attributed in the Falcondo process to use of shaft furnaces for reduction of briquetted laterite ore, where “a high degree of reduction of the ore is achieved and the subsequent electric furnace step is required to do little more than melt the reduced calcine to allow separation of the metal and slag”.²¹ Combining the high degree of reduction in the shaft furnaces with the high alloy nickel grade produced (38% Ni), the quantity of gas generation is expected to be low. Calcine permeability is another key factor for allowing gas release through the calcine burden in the furnace, and competent calcined briquettes at Falcondo would have allowed for higher permeability.

- The Cerro Matoso furnaces also stand out with low estimates of the electrode gas fluxes ($\sim 135 \text{ Nm}^3/\text{h}/\text{m}^2$). This is driven by two factors: the very high degree of pre-reduction in the rotary kiln of 90–95%,²² and the high alloy nickel grade which is produced (ranging from 37% to 46%). Stable shielded arc operation results, even with operation approaching $9 \text{ MW}/\text{m}^2$ electrode power density.
- The furnace operation at SNNC is characterized by significantly higher electrode gas fluxes than the other operations ($\sim 335 \text{ Nm}^3/\text{h}/\text{m}^2$). Operated at the full design power of 94 MW, this is predicted to be even higher, above $400 \text{ Nm}^3/\text{h}/\text{m}^2$. This is largely due to the low alloy nickel grade produced of 17–18% Ni.¹⁶ Such unusually

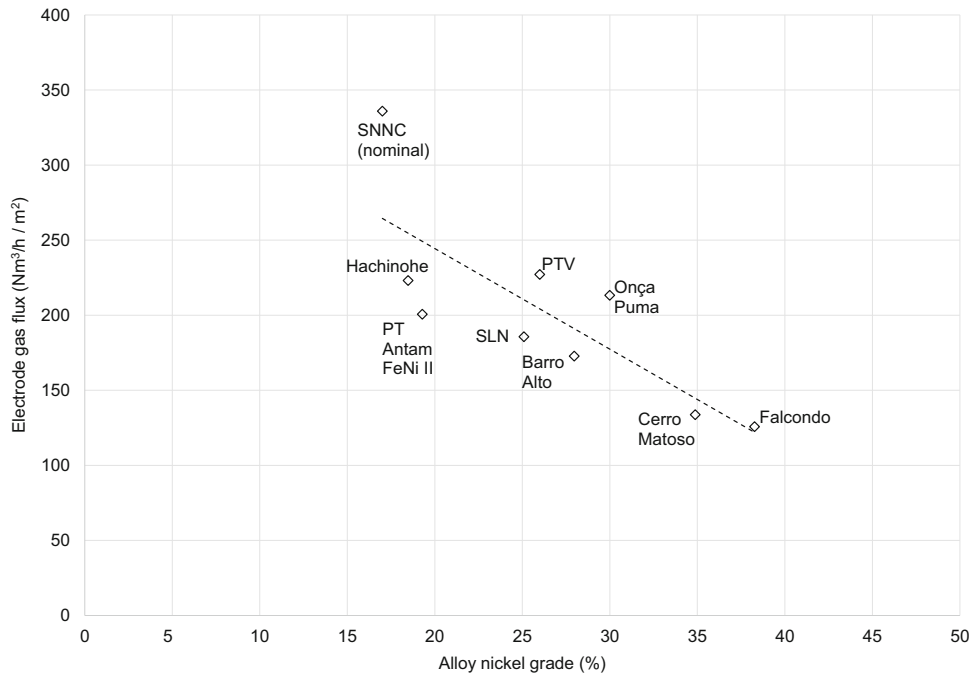


Fig. 6. Electrode gas flux ($\text{Nm}^3/\text{h}/\text{m}^2$) versus alloy nickel grade for industrial operations.

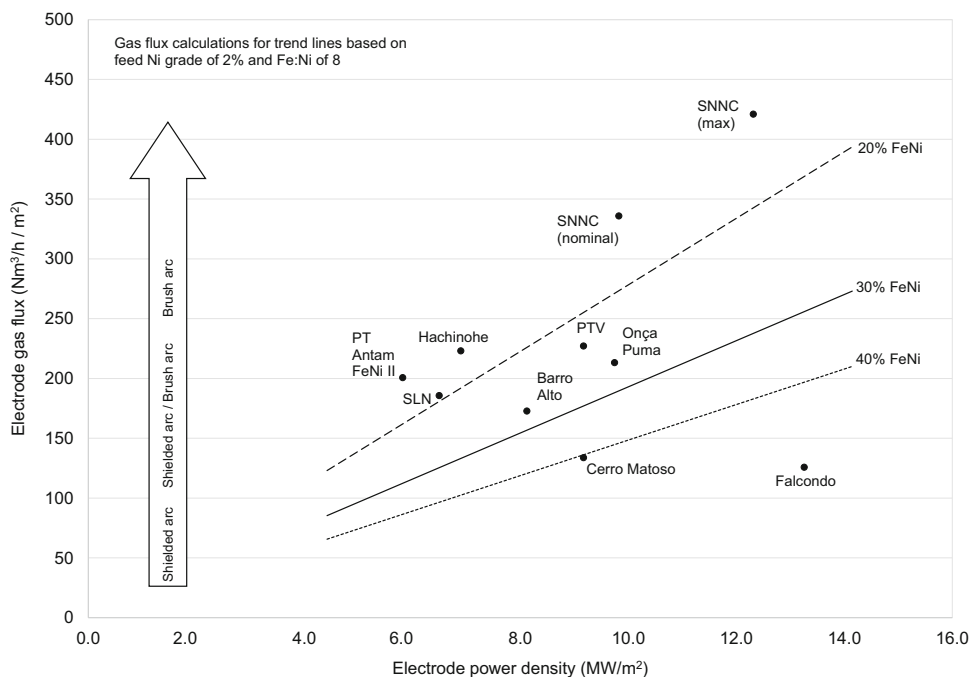


Fig. 7. Electrode gas flux ($\text{Nm}^3/\text{h}/\text{m}^2$) as a function of electrode power density for an illustrative feed nickel grade of 2% and Fe:Ni ratio of 8 and alloy nickel grades of 20%, 30% and 40%. Industrial data superimposed.

high electrode gas flux is understood to have even necessitated a switch from a shielded arc to a brush arc operation at power inputs below the 94-MW design, for risk of persistent loss of calcine burden shielding and resultant electrode electrical control and arcing instabilities. This further suggests that some limit of unacceptably high electrode gas flux has been breached, which may be inconsistent with stable shielded arc operation. This also may imply that if high electrode gas flux operation can be sustained with acceptable furnace crucible integrity and higher productivity adopting brush arc operation, potentially the perceived requirement to adopt shielded arc operation in high-intensity operation may be somewhat overstated in the industry.

- While the PT Antam FeNi II operation at Pomaala and the Pacific Metals operation at Hachinohe produce low alloy nickel grades at around 18–20%, the electrode power densities on these furnaces are low ($5\text{--}7 \text{ MW}/\text{m}^2$), thus resulting in lower electrode gas fluxes ($200\text{--}225 \text{ Nm}^3/\text{h}/\text{m}^2$). Despite this, the PT Antam operation reportedly were still operating in a brush arc mode,¹⁵ and had yet to move to a shielded arc mode.
- The Barro Alto, SLN, Onça Puma and PTV operations all produce ferronickel products in the intermediate range of 25–30%Ni grade (PTV produces a matte in the primary furnaces¹⁸), and operate with lower iron recoveries, and therefore are expected to have intermediate electrode gas

fluxes ($175\text{--}225 \text{ Nm}^3/\text{h}/\text{m}^2$). Depending on the calcine feed quality and target alloy nickel grade, operation with a stable shielded arc may prove more challenging at some limiting electrode gas flux, which, in turn, may potentially limit the realistic maximum electrode power density permissible for a continued shielded arc mode of operation.

IMPACT OF CALCINE QUALITY

The above analysis considers only generation of CO from the reduction reactions, and does not consider any other gas generation sources, or the impact of the calcine quality on the ability to shield the arc, and the resultant gas permeability. Other components in the calcine which will thermally decompose and generate gas on ignition will exacerbate the quantity of gas formed. The furnace feed particle size distribution, including any added reductant, is a critical factor for gas permeability. In the extreme, if the feed is excessively fine it may be more difficult to shield the arc, as the fine particles may simply be elutriated by the local electrode reaction gas. Ideally, larger particles with sufficient voidage between particles and of narrower particle size distribution would yield a more permeable burden for gas egress, while still containing the arc under a stable shield of calcine charge. Approaches to quantifying the impact of furnace feed size distribution and burden pressure drop have been discussed elsewhere.¹

DISCUSSION

Hearth power density has historically provided a useful metric by which to compare and scale electric furnaces, particularly in the immersed mode of electrode operation, where increased power dissipation into the slag in the furnace drives higher sidewall heat fluxes and metal temperatures. With progression to shielded arc operation, particularly in the ferronickel industry, the power dissipated in the arc zone partially offsets the power dissipated in the slag zone, thus reducing sidewall heat fluxes and metal temperatures. On this basis, the liquid zone (metal and slag zones) of the crucibles in shielded arc operation are subject to less arduous conditions; however, the intensity of the furnace operation is then shifted to the electrodes. Therefore, closer attention is required to factors such as the local electrode gas fluxes (or superficial gas velocities), freeboard and off-gas temperatures, for any given calcine feed quality, and so optimal extent of electric furnace reduction and its resultant alloy nickel grade and overall nickel recovery.

CONCLUSION

In further scale-up of ferronickel electric smelting furnaces, it is considered that the hearth power density, while extremely important for the liquid crucible region of the furnace, may not be particularly instructive about the conditions local to the electrodes when operated in shielded arc mode. Defining the ratio of arc power to bath power,⁴ while improving on local electrode characterization and providing some quantitative electrical measure of the extent of arc shielding, fails to account adequately for the impact of overall local electrode and process dynamics, and so the conditions that affect the presence, or absence, of calcine burden shielding the arc. An approach to quantifying the electrode gas flux has been suggested above, providing an improved link between ferronickel calcine feed characteristics, the product alloy nickel grade and the electrode power density metric, as a means to define conditions capable of securing stable shielded arc operation. While there are aspirations to design and operate ferronickel furnaces at substantially higher than 100 MW, further understanding of the local electrode conditions is required to help better guide on scale-up potential, especially in terms of:

- Local electrode gas flux permissible at a given maximum electrode power density to safely sustain stable shielded arc operation;
- Potential to forego shielded arc operation entirely for brush, or possibly even open, arc operation to permit still higher electrode power density (without the attendant operational instabilities attributable to variable calcine cover of an arc), yet while still critically achieving all essential furnace integrity and longevity.

ACKNOWLEDGEMENTS

The authors hereby express their gratitude to Anglo American and Anglo American Platinum for permission to publish this paper.

REFERENCES

1. L.R. Nelson, in *EPD Congr. 2014, Proc. Symp.* (San Diego, California, USA, 16–20 Feb 2014) pp. 39–68.
2. C. Walker, S. Kashani-Nejad, A.D. Dalvi, N. Voermann, I.M. Candy, and B. Wasmund, in *Annu. Conf. Metall. CIM, 48th, 2009* (Sudbury, ON, Canada, 23–26 Aug 2009), pp. 33–50.
3. F.R. Archibald and G.G. Hatch, U.S. Patent 3,715,200 (1973).
4. N. Voermann, T. Gerritsen, I. Candy, F. Stober, and A. Matyas, in *Int. Laterite Nickel Symp., Proc. Symp.* (Charlotte, North Carolina, USA, 14–18 March 2004), pp. 563–577.
5. A.E.M. Warner, C.M. Diaz, A.D. Dalvi, P.J. Mackey, and A.V. Tarasov, *JOM* 3, 11 (2006).
6. M. Jastrzebski, T. Koehler, K. Wallace, N.V. Novikov, N. Novikov, B. Zaporozhets, D. Shevchenko, N. Kryzhanovskaya, and I. Kapran, in *Annu. Conf. Metall. CIM, 51st, 2012* (Niagara, ON, Canada, 30 Sep–3 Oct 2012), pp. 29–41.
7. F. Stober, T. Miraza, A. Taofik Hidayat, I. Jauhari, K. Said, N. Voermann, B.O. Wasmund, C. Nichols, K. Belanger, D. Fowler, and T. Gerritsen, A. Matyas, in *Int. Ferro-Alloys Congr., 11th* (India, 2007), pp. 638–653.
8. L.R. Nelson, R.J. Hundermark, and K. van der Merwe, *Annu. Conf. Metall. CIM, 54th, 2015* (Toronto, Canada, 23–26 Aug 2015) Paper 8877.
9. E.W. Lithgow and J.H. Corrigan, in *Extr. Metall. Copper, Nickel Cobalt, Proc. Paul E. Queneau Int. Symp.*, TMS (Denver, Colorado, Feb 1993), pp. 427–440.
10. M.Y. Solar, I. Candy, and B. Wasmund, *CIM Bull.* 11, 1107 (2008).
11. M.Y. Solar, S. Mostaghel, and S. Nicol, in *Annu. Conf. Metall. CIM, 53rd, 2014* (Vancouver, BC, Canada, 28 Sep–1 Oct 2014), Paper 8626.
12. R.T. Jones, G.M. Denton, Q.G. Reynolds, J.A.L. Parker, and G.J.J. Van Tonder, *J. South Afr. Inst. Min. Metall.* 102, 5 (2002).
13. R.T. Jones, *Proc. EMC 2013* (Weimar, Germany, 23–26 June 2013), pp. 1019–1025.
14. D.R. Swinbourne, *Trans. Inst. Min Metall., Sect. C*, 123, 3, 127 (2014).
15. L.R. Nelson, J.M.A. Geldenhuis, T. Miraza, T. Badrujman, A. Taofik Hidayat, I. Jauhari, F.A. Stober, N. Voermann, B.O. Wasmund, and E.J.M. Jahnsen, in *Int. Ferro-Alloys Congr., 11th* (India, 2007), pp. 798–813.
16. L. Rodd, N. Voermann, F. Stober, B.O. Wasmund, S.H. Lee, K.Y. Lim, J.-H. Yoo, S.-J. Roh, and J.-H. Park, in *Int. Ferro-Alloys Congr., 12th* (Helsinki, Finland, 6–9 June 2010), pp. 697–708.
17. C. Walker, T. Koehler, N. Voermann, and B. Wasmund, *Int. Ferro-Alloys Congr., 12th* (Helsinki, Finland, 6–9 June 2010), pp. 681–696.
18. C. Doyle, *Int. Laterite Nickel Symp., Proc. Symp.* (Charlotte, North Carolina, USA, 14–18 March 2004), pp. 667–684.
19. M.S. Rennie, *Mintek 50: Proc. Int. Conf.* (Sandton, South Africa, 1984), pp. 777–785.
20. R.C. Urquhart, *Annu. Conf. Metall. CIM, 53rd, 2014* (Vancouver, BC, Canada, 28 Sep–1 Oct 2014), Paper 8660.
21. D.G.E. Kerfoot, *Ullmann's Encyclopedia of Industrial Chemistry* (Weinheim: Wiley-VCH Verlag GmbH & Co. KGaA, 2010), pp. 37–101.
22. J.R. Kift and C.E. Ferrer, in *Int. Laterite Nickel Symp., Proc. Symp.* (Charlotte, North Carolina, USA, 14–18 March 2004), pp. 719–731.